P5.8

DEVELOPMENT OF A NEW C-BAND BISTATIC POLARIMETRIC RADAR AND OBSERVATION OF TYPHOON EVENTS

Katsuhiro NAKAGAWA, Hiroshi HANADO, Shinsuke SATOH, Nobuhiro TAKAHASHI,
Toshio IGUCHI, and Kouichi FUKUTANI
Communications Research Laboratory, Okinawa, Japan

1. INTRODUCTION

Each year in Japan, precipitation phenomena - such as localized torrential rain, typhoons, and heavy snow - inundate homes, cause mudslides, and damage crops. These natural disasters lead to loss of life and destroy valuable property. Such precipitation events are typical examples of meso-scale atmospheric phenomena, which occur on scales ranging from several kilometers to several hundred kilometers and last from several minutes to several days. The precipitation radar is a remote-sensing instrument that can be used to instantaneously and continuously observe an extremely wide area (with a radius of several hundred kilometers) from a single point on the ground. Therefore, it represents an effective tool in monitoring and understanding the mechanisms of such meso-scale phenomena. A conventional precipitation radar emits radio waves from the ground toward the sky and then receives the backscattered signals. The precipitation intensity can be derived from the intensity of the received signal.

Communications Research Laboratory (CRL) has developed a new C-band multi-parameter Doppler radar system with a bistatic Doppler radar network. This new radar is named COBRA (CRL Okinawa bistatic polarimetric radar). The weather targets of the system are typhoons, Baiu-frontal rainfall, meso-scale precipitation in subtropical zones, and clear-air turbulence. Our goal is to utilize COBRA in developing meso-scale meteorological and hydrological observation applications to support commercial weather forecasting and data collection for disaster prevention purposes.

2. COBRA SYSTEM

The COBRA system features a main radar with polarization measurement functions to enable detailed observation of the polarization characteristics of precipitation particles. It also employs a bistatic radar networkó specifically, a network of receivers for observing oblique scattering from precipitation particles. Fig. 1 shows the locations of all the equipment in COBRA. The main radar is located at the Nago precipitation radar facility in Nago, Okinawa (CRL Nago). The bistatic receiver stations are located at the Ogimi wind profiler facility (CRL Ogimi) and at CRL Okinawa. The two bistatic radar stations are connected to CRL Nago by a dedicated line with a throughput of 128 kbps, while CRL Nago and CRL Okinawa are also linked by a dedicated line operating at 100 Mbps. CRL Nago is unmanned; it is remotely controlled and monitored from CRL Okinawa.

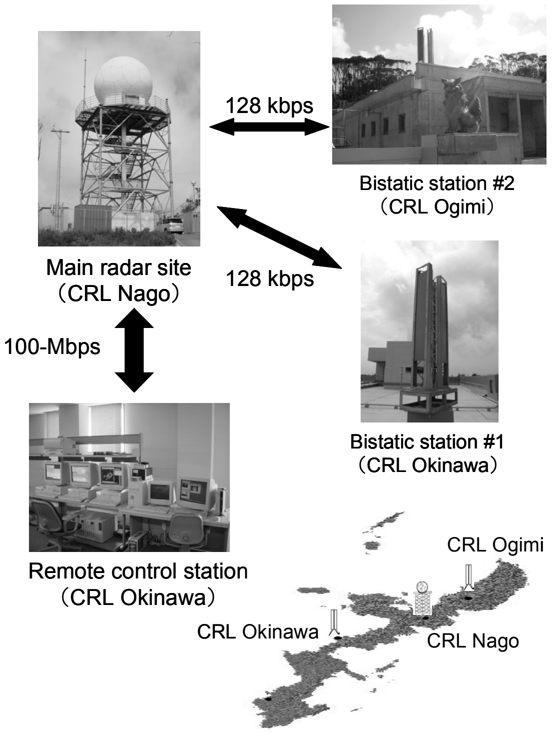

Fig. 1 Installation locations and network links of the COBRA system.

2.1 *Main Radar*

The main radar of the COBRA system is a ground-based, monostatic pulse Doppler radar using a single wave (5340 MHz) in the C-band. Its main specifications are listed in Table 1. The maximum observation range is a radius of approximately 300 km, although this depends on the repetition frequency and the transmitted pulse. The spatial resolution is 37.5ñ600 m, depending on the pulse width and the over-sampling rate. To enable polarimetric observations, an antenna with a good side-lobe level and cross-polarization ratio and a radome with little attenuation were selected. Two transmitter (klystron)

**Corresponding author address*:
Katsuhiro NAKAGAWA, Okinawa Subtropical Environment Remote-sensing Center, Communications Research Laboratory, 4484 Aza-Onna, Onna, Kunigami, Okinawa 904-0411, Japan; e-mail: nakagawa@crl.go.jp.

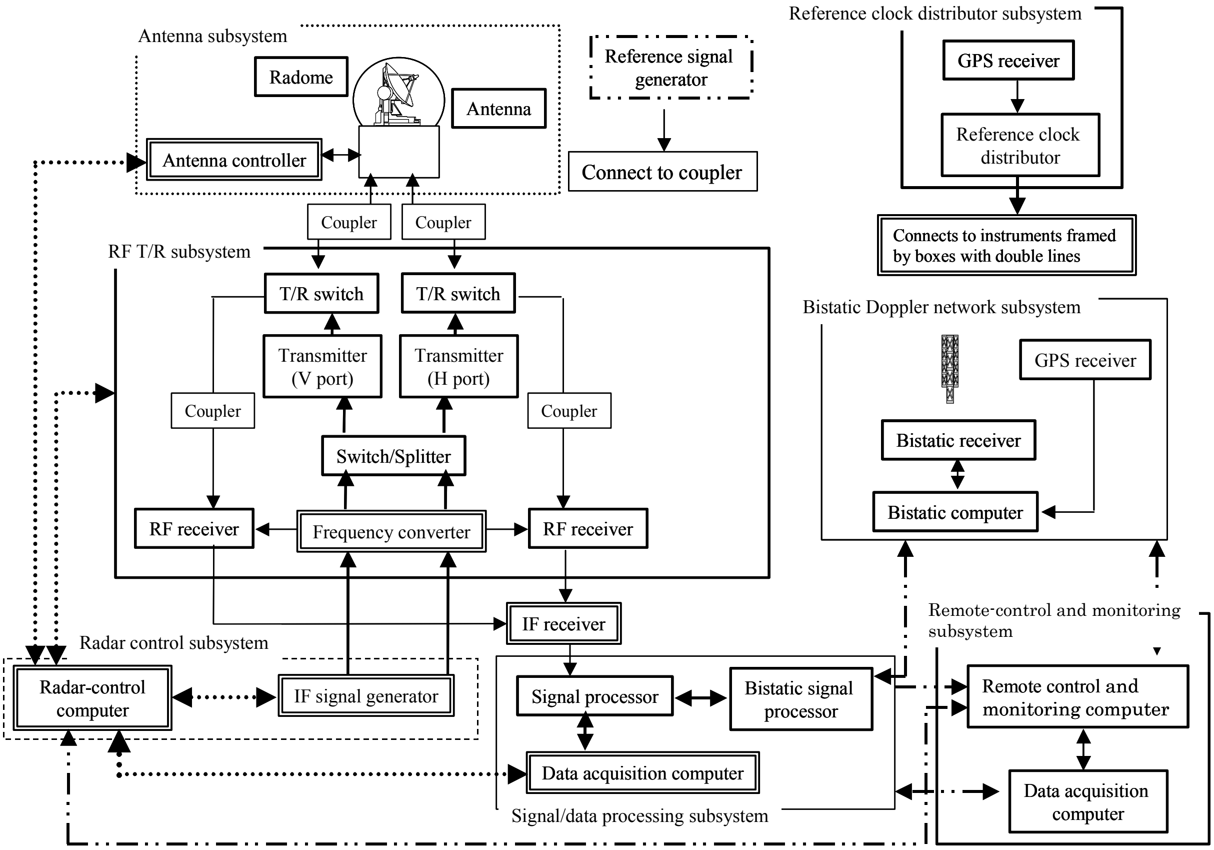

Fig. 2 Block diagram of COBRA. The solid and dotted lines represent the flow of radar signals and control signals, respectively. The lines of alternating dashes and double dots show the flow of data in the network.

units are used to observe polarization. The transmission polarization for each pulse is selected from six possible polarizations: horizontal polarization, vertical polarization, ±45-degree-tilt linear polarizations, and right- and left-handed circular polarizations. The return signal is measured simultaneously by two receivers, one for the horizontal polarization and the other for the vertical polarization (Fig. 2). The pulse width can be adjusted to 0.5, 1.0, or 2.0 μs. The system is controlled by a GPS signal with a 10-MHz clock, and the operation of the bistatic Doppler network is fully synchronized by using this GPS signal.

Doppler observation can be performed in two modes: pulse-pair observation, for measuring the Doppler velocity and spectral width; and FFT observation, for measuring the Doppler spectrum. To correct for Doppler velocity folding, the system can be set to switch the double PRF between pulses.

2.2 *Bistatic Doppler Network*

Doppler observations are made with the COBRA main radar to observe the background winds occurring with precipitation. By combining this information with the results of Doppler-shift measurements of oblique scattering from precipitation particles, which are made by the two bistatic receiver units, it is possible to observe 3-D wind speed fields quickly and with precision over a wide area (J. Wurman et al. 1993).

Relative to conventional dual observation with a combination of two or three monostatic Doppler radars, the advantages of the bistatic radar network lie in its lower cost and greater simplicity. Furthermore, the process of acquiring 3-D data over a wide area by perfect synchronous measurement using dual-mode observation is time-consuming, since the measurements are made with narrow-beam radars. Measurements taken without complete synchronicity are not sufficiently reliable for observing meso-scale meteorological phenomena displaying large temporal variations. With the bistatic method, however, perfect synchronicity is guaranteed, since signals from the irradiated part of the main radar are received simultaneously by all receivers, so data acquisition can be performed in a short time. In addition, using two or three monostatic Doppler radars for dual observation requires two or three frequencies in the C-band; the bistatic radar network, however, requires only one frequency, enabling more effective use of bandwidth.

2.3 *Signal Processing*

The measured signals are categorized into three processing levelsó Level 1, Level 2, and Level 3ó and are processed in real time. Figure 3 shows a block diagram of the signal and data flow.

TABLE 1 Specifications of the COBRA system

Frequency	5340 MHz (C-band)
Peak Power	250 kW◊2 (Dual Klystron)
Pulse width	0.5, 1.0, 2.0 μs
PRF	250-3000 Hz, 1-Hz step
Antenna	4.5-m Φ parabola (8-m Φ radome)
Antenna gain	45.6 dBi (H) / 45.7 dBi (V) (include radome)
Beam width	0.91 deg (H) / 0.91 deg (V)
Sidelobe level	< -31.8 dB (AZ), < -28.3 dB (EL)
Cross pol ratio	39.2 dB (H) / 40.3 dB (V) (integ in a beam)
Doppler estimation	Pulse-pair / FFT
Range bin num	> 2000 bin
Antenna scan	PPI : 0.5-10 rpm, 0.1-rpm step RHI : 0.1-3.6 rpm, 0.1-rpm step

(a) *Level-1 Processing*: In Level-1 processing, the received horizontal and vertical polarization signals (input) are processed to determine: (1) the Stokes parameters of the transmitted and received signals for fully polarimetric observation (G. G. Stokes 1852); (2) the complex cross-correlation for the pulse-pair method; (3) the Doppler spectrum, obtained by FFT; and (4) the noise levels of the two receivers for both horizontal and vertical signals. The results are stored as Level-1 processed data.

(b) *Level-2 Processing*: In Level-2 processing, the precipitation intensity, R, is calculated from its Z-R relationship with the radar reflectivity factor, Z. In addition, polarization parameters are calculated, including the differential reflectivity between the horizontal and vertical polarizations, ZDR (=ZHH/ZVV), the linear depolarization ratio, LDR (=ZHV/ZHH), the cross-correlation coefficient, ρHV(0), and the differential propagation phase between the horizontal and vertical polarizations, ΦDP (and its derivative in the range direction, KDP). Based on these data, the forms of precipitation particles can be identified and the raindrop size distribution estimated (R. J. Doviak et al. 1993; H. Kumagai et al. 1993). Wind-speed vector data acquired by the bistatic radar network is also processed, and the precipitation intensity is estimated by using the ZDR, KDP, and k-R relationships, as well as the standard Z-R relationship (T. A. Seliga et al. 1976; M. Sachidananda et al 1986; V. N. Bringi et al. 2001). These data are stored as Level-2 processed data.

(c) *Level-3 Processing*: In Level-3 processing, the precipitation intensity, R, which is initially handled as Level-2 data, is statistically analyzed to determine such items as the 1-hr accumulated precipitation, 1-hr average precipitation, 24-hr accumulated precipitation, 24-hr average precipitation, 48-hr accumulated precipitation, and 48-hr average precipitation. To support disaster-prevention activities, the 1-hr accumulated precipitation, 1-hr average precipitation, and 24-hr accumulated precipitation are determined for the drainage areas around the dams on the main island of Okinawa. The resulting data are then publicized in real time on the Web as image data, including video.

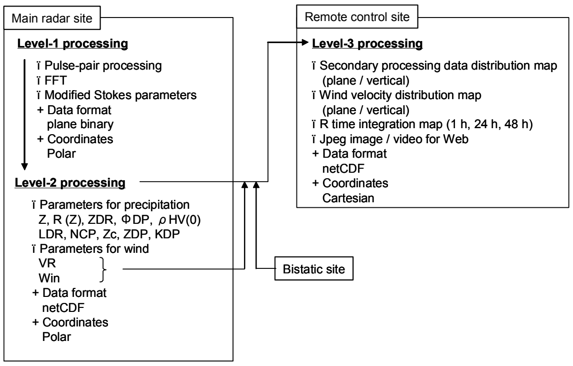

Fig. 3 Block diagram of the signal and data flow

3. OBSERVATION RESULTS

The COBRA system was used to observe two typhoon events, Typhoon Ramasun and Typhoon Shinraku, in 2002. A synchronous observation with the TRMM/PR was performed in the case of Typhoon Ramasun. We could thus verify the performance of COBRA by comparing the synchronous data from TRMM/PR.) Fig. 4 shows a comparison of the radar reflectivity observed by each system. In this case, TRMM passed through sky above the radar site for 10 minutes during the middle of the volume scan (14:35-14:44 UT). Horizontal matching of the COBRA and TRMM/PR data was performed by using the echo patterns of isolated echoes or scanning edges. The results show that the radar reflectivity observed by TRMM/PR and that observed by COBRA were well in agreement. The offset in this is about 0.5 dB.

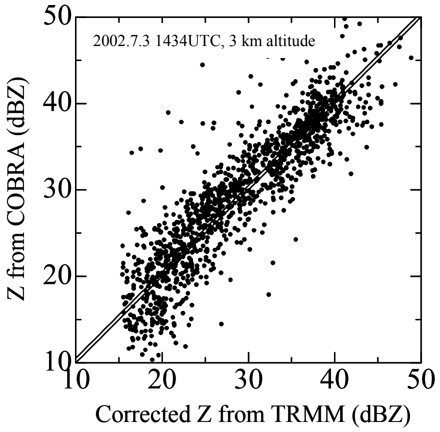

Fig. 4 Comparison of the radar reflectivity of TRMM/PR and COBRA at an altitude of 3 km for Typhoon Ramasun. The TRMM/PR data was retrieved by algorithm 2A25. The COBRA data is the mean average value within the footprint of TRMM/PR.

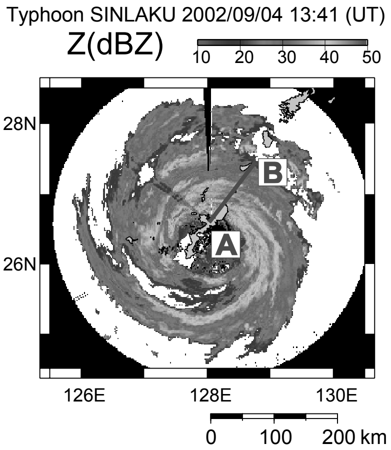

Fig. 5 Horizontal distribution of the radar reflectivity factor of Typhoon Shinraku, observed at 13:41 on September 4, 2002 (UT). (Elevation = 0.4 deg)

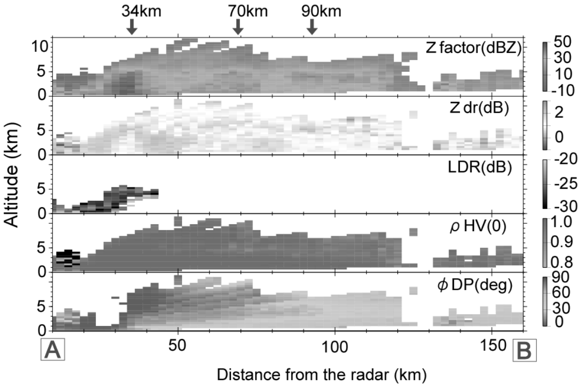

Fig. 6 Polarimetric observations of rainfall in the vertical distribution of section A-B in Fig. 5.

Fig. 5 shows the horizontal distribution of the radar reflectivity factor of Typhoon Shinraku, observed at 13:41 on Sept. 4, 2002 (UT). Detailed rain structures, such as the eye of the typhoon and a rain region in the shape of a swirl of the circumference, were clearly observed. Figure 6 shows polarimetric observations of the rainfall along the vertical section A-B in Fig. 5. In Fig. 6, the top plate shows the radar reflectivity factor, ZHH. Strong rain band areas existed at horizontal distances of 34, 70, and about 90 km from the radar. The second plate from the top shows the differential reflectivity, ZDR, which results from the flattening of raindrops due to their motion relative to the air. Comparison among the rain band areas at 34, 70, and 90 km suggests that those at 70 km and near 90 km contained bigger raindrops than did the band near 34 km. The middle plate shows the linear depolarization ratio, LDR. Although this figure is limited to a radius of 50 km from the radar, the detailed structure inside a rain band, which could not be determined from the distribution of the radar reflectivity factor, could be observed. The second plate from the bottom shows the cross-correlation coefficient, ρHV(0). In the rain bands at 70 km and near 90 km, ρHV(0) had a small value of about 0.8. This suggests that a melting layer existed around an altitude of 4-5 km. The bottom plate shows the differential propagation phase between the horizontal and vertical polarizations, ΦDP. The value increased as the distance from the radar became longer, and ΦDP was also large in areas where the value of ZDR was large.

4. SUMMARY

The installation of the COBRA system has been completed, and performance tests on the main radar are currently being conducted, along with an operational check of the bistatic Doppler network and various system performance tests. As an experimental observation, COBRA was used to observe two typhoon events, Typhoon Ramasun and Typhoon Shinraku, in 2002.

The polarization observation data collected by the COBRA main radar will be validated by using the 400-MHz wind profiler (T. Adachi et al. 2001) and ground-based precipitation observation data at CRL Ogimi. Ground-based raindrop-size distribution measurements will be made using a Joss-disdrometer and a 2-dimensional video disdrometer. An optical rain gauge (which can measure the 1-minute precipitation intensity) and a tipping-bucket rain gauge will also be used for observations of precipitation intensity.

5. REFERENCES

J. Wurman, S. Heckman, and D. Boccippio, 1993: A Bistatic Multiple-Doppler Radar Network.
J. Appl. Meteorol., **32** , 1802-1814

G. G. Stokes, 1852: On the composition and resolution of streams of polarized light from different sources.
Trans, Comb. Phil. Soc., **9**, 399-416

R. J. Doviak and D. S. Zrnic, 1993: Doppler radar and weather observations.
2nd ed., Chaps. 6 and 8, Academic Press

H. Kumagai, R. Meneghini, and T. Kozu, 1993: Preliminary results from multparameter airborne rain radar measurement in the Western Pacific.
J. Appl. Meteorol., **32**, 431-440

T. A. Seliga and V. N. Bringi, 1976: Potential use of radar differential reflectivity measurements at orthogonal polarizations for measuring precipitation.
J. Appl. Meteorol., **15**, 69-76

M. Sachidananda and D. S. Zrnic, 1986: Differential propagation phase shift and rainfall rate estimation.
Radio Sci., **21**, 23-247

V. N. Bringi and V. Chandrasekar, 2001: Polarimetric Doppler Weather Radar ñ Principiles and applications ñ.
Cambridge University Press

T. Adachi, Y. Masuda, and S. Fujii, 2001: Development of a 400MHz-band Wind Profiler Radar in Okinawa.
The third International Sympo. on Asian Monsoon System (ISAM3), 309-313